



ELSEVIER

Contents lists available at ScienceDirect

European Journal of Pharmacology

journal homepage: www.elsevier.com/locate/ejphar

Molecular and cellular pharmacology

Epigallocatechin-3 gallate inhibits cancer invasion by repressing functional invadopodia formation in oral squamous cell carcinoma

Young Sun Hwang^{a,*}, Kwang-Kyun Park^{b,c,d}, Won-Yoon Chung^{b,c,d,**}^a Department of Dental Hygiene, College of Health Science, Eulji University, 212 Yangji-dong, Sujeong-gu, Seongnam 461-713, Republic of Korea^b Oral Cancer Research Institute, Yonsei University College of Dentistry, Republic of Korea^c Department of Oral Biology, Yonsei University College of Dentistry, Republic of Korea^d The Applied Life Sciences, Graduate School, Yonsei University College of Dentistry, Republic of Korea

ARTICLE INFO

Article history:

Received 3 January 2013

Received in revised form

25 April 2013

Accepted 5 May 2013

Available online 22 May 2013

Keywords:

EGCG

Invadopodia formation

Src

Cortactin

FAK

RhoA activation

ABSTRACT

Although the polyphenol EGCG has various beneficial biological effects, its effect on cytoskeletal activities during cancer invasion is not well defined, and the precise molecular mechanisms are largely unknown. Here, we provide molecular evidence on the anti-invasion effect of EGCG in OSCC cells using an *in vitro* 3-D culture system and *in vivo* athymic mouse model. Briefly, EGCG exerted an inhibitory effect on the Matrigel-based Transwell invasion and migration of OSCC cells. These effects were not due to decreased cell viability or adhesion capacity to ECM. EGCG-treated OSCC cells possessed fully extended actin fibers without invadopodia, indicating a loss of ECM degradation capacity. Decreased phosphorylation of Src, CTTN, and FAK also followed EGCG treatment. Additionally, EGCG reduced activation of RhoA in dominant-negative RhoA N19 and constitutively active RhoA Q63E cells, and inhibited the invasive capability of these cells in the 3-D cell growth model. Furthermore, the administration of EGCG led to substantial inhibition of tumor growth and activation of invadopodial proteins in the tumor tissues of mice inoculated with OSCC cells. The data indicate the potential value of EGCG as an invadopodia-targeted anti-invasive agent in cancer therapy.

© 2013 Elsevier B.V. All rights reserved.

1. Introduction

Cancer invasion is an important step in the metastatic dissemination of cancer cells. This step involves remodeling of the extracellular matrix (ECM) and cell-matrix interaction, cell movement mediated by the actin cytoskeleton, and activation of focal adhesion kinase (FAK)/Src signaling (Murphy and Courtneidge, 2011). Growing evidence suggests that cancer cell invasion is mediated by invadopodia, which are primary sites of rapid actin polymerization distinct from focal adhesions (Ridley, 2011). Invadopodia is an actin-based membrane protrusion formed at contact sites between invasive tumor cells and the ECM with focal ECM degradation capacity (Buccione et al., 2009). Epidemiological studies suggest that the metastatic behavior of cancer may be an ideal target for chemoprevention. Thus, a better understanding of the mechanisms underlying the forms and functions of invadopodia should facilitate identification of novel targets for anti-invasive therapy as a model for drug discovery. Moreover, because the

turnover of constituent molecules is extremely rapid and they are rapidly disassembled after application, invadopodia are not critical for overall cell viability (Weaver, 2006). Consequently, anti-invadopodia therapy as therapeutic target would be expected to have fewer side effects than chemo- and radio-therapy approaches. This type of approach has the added advantage of potentially accelerating the biological discovery process.

Persuasive epidemiological and experimental evidence suggests that a phytochemical-enriched diet may aid in preventing many cancers (Mukhtar and Ahmad, 1999) including oral cancer (Chen et al., 2011). Epigallocatechin-3 gallate (EGCG) targets multiple signaling pathways including microRNA (miRNA), one of the mechanisms for cells to achieve subtle change in multiple targets (Khan et al., 2006; H. Wang et al., 2011). However, although EGCG exhibits beneficial effects, its effect on cytoskeletal activities is not well understood. Although anti-invasion and anti-tumor activity of EGCG has been recently reported in oral cancer (Chen et al., 2011), little is known of how EGCG perturbs tumor invasion at the cytoskeletal level, like functional invadopodia. Moreover, active RhoA, which is prominent at the leading edge of protrusion, has not been considered.

Presently, we demonstrate that EGCG represses functional invadopodia formation by inhibition activation of Src, FAK, cortactin (CTTN), and RhoA in oral squamous cell carcinoma (OSCC) cells,

* Corresponding author. Tel.: +82 31 740 7493; fax: +82 31 740 7352.

** Corresponding author at: Oral Cancer Research Institute, Yonsei University College of Dentistry, Republic of Korea. Tel.: +82 2 2228 3057; fax: +82 2 364 7113.

E-mail addresses: kiteys@eulji.ac.kr (Y.S. Hwang), wychung@yuhs.ac (W.-Y. Chung).

resulting in the inhibited migration and invasion of OSCC cells *in vitro*, and cancer growth and regional infiltration of OSCC cells *in vivo*.

2. Material and methods

2.1. Plasmid

To generate the dominant-negative and constitutively active human RhoA mutant vectors, RhoA N19 and RhoA Q63E mutants were constructed by a polymerase chain reaction (PCR)-based point mutation method using the Ultimate™ ORF Clones (#Clone ID; IOH7574, Invitrogen Co., New York, USA) as a template, followed by subcloning into the pcDNA3.1 mammalian expression vector (Invitrogen) to generate the stable cell line. To confirm the RhoA mutation (T19N and Q63E), the RhoA N19/pcDNA3.1 and RhoA Q63E/pcDNA3.1 plasmids were subjected to DNA sequencing analysis. The pcDNA3.1 vector without the inserted gene was used for the control stable cell line (Mock).

2.2. Cell culture

OSCC cells were cultured in Dulbecco's modified Eagle's medium (DMEM)/Ham's F-12 nutrient mixture (3:1 ratio) medium supplemented with 10% fetal bovine serum (FBS), 1×10^{-10} M cholera toxin, 0.4 mg/ml hydrocortisone, 5 µg/ml insulin, 5 µg/ml transferrin and 2×10^{-11} M triiodothyronine (T3) in a humidified atmosphere of 5% CO₂ at 37 °C. The stable cell lines were created without clonal selection by LipofectAMINE-mediated transfection of the entire population of OSCC cells with a dominant negative RhoA N19 expression plasmid, constitutively active RhoA Q63E expression plasmid, or with the pcDNA 3.1 control vector (Mock) followed by continual selection with 1.5 mg/ml G418 (Gibco BRL Co., Rockville, MD, USA). G418-resistant clones were expanded to cell lines and used to produce the stable cell lines.

2.3. Transwell® invasion assay

Cells were cultured in complete medium in the presence of [³H]-thymidine (10 µCi/ml) for 24 h and then harvested and washed with culture medium. Polycarbonate nucleopore filter inserts with a pore size of 8 µm in a 24-well Transwell chamber (Corning Costar, Cambridge, MA, USA) were coated with Matrigel (30 µg/well; Becton Dickinson, Lincoln Park, NJ, USA). The [³H] thymidine-labeled cells (5×10^4 cells) were seeded into the upper part of the Matrigel-coated filter, complete medium with EGCG was added to the lower portion, and the cells were incubated for 48 h. The radioactivity of the cells that invaded through the Matrigel into the lower chamber was assessed with a LS6500 Liquid Scintillation Counter using a liquid scintillation cocktail (Beckman Colter, Fullerton, CA, USA). Results are expressed in terms of the changes in invasion relative to the controls (Hwang et al., 2006).

2.4. Antibodies

Alexa fluor 568 phalloidin antibody was purchased from Invitrogen. Cortactin (clone 4F) was purchased from Millipore (Billerica, MA). Anti-cortactin (phospho Y466) antibody was from Abcam (Cambridge, MA, USA). Src antibody, phospho-Src family (Tyr416) antibody, FAK antibody, and phospho-FAK (Y397) antibody were purchased from Cell Signaling Technology (Beverly, MA, USA). RhoA was acquired from Santa Cruz Biotechnology (Santa Cruz, CA, USA). Horseradish peroxidase-conjugated secondary antibodies were purchased from Amersham Life Science (Little

Chalfont, UK). Fluorescein isothiocyanate (FITC)-goat anti-mouse IgG (H+L) and FITC-goat anti-rabbit IgG (H+L) antibodies were purchased from Zymed (San Francisco, CA, USA).

2.5. ECM cell adhesion assay

The ECM cell adhesion assay was carried out with an ECM Cell Adhesion Array kit (Colorimetric, Chemicon International, Temecula, CA, USA). Collagen I, collagen II, collagen IV, fibronectin, laminin, tenascin, and vitronectin were pre-coated onto 96-well microtiter plates arranged in 12 × 8-well strips. One bovine serum albumin (BSA)-coated well in each 8-well strip served as a negative control. Briefly, the plate strips were rehydrated with PBS for 10 min at room temperature. Cells were washed with serum-free medium after quenching the trypsin with soybean trypsin inhibitor (1 mg/ml). The cell suspension in complete media (5×10^5 cells) was seeded onto the ECM-coated substrates and incubated for 2 h at 37 °C in a CO₂ incubator. After discarding the medium from the wells and washing with assay buffer, the cells were incubated with cell staining solution for 5 min at room temperature and completely solubilized with extraction buffer. The ability of the cells to bind to the respective ECM proteins was analyzed using a microplate reader at 540 nm.

2.6. Cell viability

Cells (5×10^3 cells/well) were plated in a 96-well culture plate with complete medium and left overnight to adhere. The cells were treated with EGCG (Sigma Chemical Co., St Louis, MO, USA) for indicated time and then incubated with a 3-(4,5-Dimethylthiazol-2-yl)2,4-diphenyl tetrazolium bromide (MTT) solution (5 mg/ml) for an additional 4 h at 37 °C. The medium was carefully removed and the formazan product was dissolved with 200 µl dimethyl sulfoxide (DMSO). Absorbance was measured at 570 nm on a microplate reader (Bio-Rad, Hercules, CA, USA).

2.7. Invadopodia formation

Cells (1×10^3 /ml) were plated on gelatin-coated chamber slides and cultured for 6 h. The floating cells were aspirated and the remaining cells were fixed in 4% paraformaldehyde followed by permeabilization with 0.5% Triton X-100/PBS and staining with anti-CTTN antibody and Alexa fluor 568 phalloidin. FITC-goat anti-mouse IgG (H+L) was used as the secondary antibody for anti-CTTN. The cells were visualized and photographed with a LSM 510 META confocal laser-scanning microscope (Carl Zeiss, Jena Germany). Images were processed using Zeiss LSM image browser software. Invadopodia were identified as regions of CTTN-containing actin spots.

2.8. ECM degradation assay

FITC-conjugated gelatin-coated coverslips were prepared as described previously (Bowden et al., 2001). Oregon Green 488 gelatin was purchased from Molecular Probes (Carlsbad, CA, USA). Gelatin-coated coverslips were quenched for 1 h with serum-containing media at 37 °C prior to cell plating. To evaluate invadopodia formation and FITC-gelatin matrix degradation, cells were plated on FITC-conjugated gelatin-coated coverslips in 12-well plates at 4×10^3 /ml and cultured for 16 h. Cells were fixed with 4% paraformaldehyde followed by permeabilization with 0.5% Triton X-100/PBS and stained for actin with Alexa fluor 568 phalloidin. Foci of the degraded matrix were visible as dark areas lacking fluorescence and appeared as 'holes' in the string fluorescence gelatin matrix. The gelatin matrix and actin-stained cells were photographed using a LSM 510 META confocal laser-scanning

microscope (Carl Zeiss). Images were processed using Zeiss LSM image browser software.

2.9. Western blotting

Equal quantities of protein (50 µg) were separated on 10% sodium dodecyl sulfate (SDS)-polyacrylamide gels and the proteins were transferred to a polyvinylidene difluoride membrane (Millipore). The membrane was blocked with 10% skim milk in PBS containing 0.1% Tween-20 (PBS-T) and subsequently incubated with a 1:1000 dilution of each primary antibody against specific proteins in 10% skim milk overnight at 4 °C. The blots were incubated with a 1:3000 dilution of the respective horseradish peroxidase-conjugated secondary antibodies for 2 h at room temperature and were washed again with PBS-T. The targeted proteins were visualized using an Enhanced Chemiluminescence Detection kit (Amersham Life Science, Parsippany, NJ, USA), according to the manufacturer's protocols.

2.10. Gelatin zymography

Cells were plated in 1% serum-containing medium and cultured for 24 h. The conditioned medium was collected and protein concentrations were determined by the Bradford method (Bio-Rad). Equal quantities of protein (10 µg) were separated on 8% SDS-PAGE containing 0.1% (w/v) gelatin. The gels were washed with 2.5% Triton X-100 for 30 min at room temperature and then incubated in a buffer containing 10 mM CaCl₂, 0.01% NaN₃ and 50 mM Tris-HCl (pH 7.5) for 16 h at 37 °C. The gel was stained with 0.2% Coomassie Brilliant Blue and photographed on a light box. Gelatinolytic activity of the matrix metalloproteinases (MMPs) was detected as clear bands on a dark blue background.

2.11. Cell membrane extraction and collagen zymography

Cell membrane fractions were prepared by resuspending cells in ice-cold DIG buffer I comprised of 0.1% digitonin, 0.5 M NaCl, 20 mM HEPES (pH 7.0) for 10 min. Unlysed cells were harvested by centrifugation for 5 min at 1000 rpm. After three rinses with DIG buffer I, the final pellet was resuspended in DIG buffer II [1% digitonin, 0.15 M NaCl, 20 mM HEPES (pH 7.0)] for 2 h on ice with gentle motion to extract membrane proteins. The supernatant was collected following centrifugation for 5 min at 1000 rpm and represented the membrane fraction. To study the effect of EGCG on MT-MMP collagenolytic activity, equal quantities of protein (10 µg) were loaded and separated by 10% SDS-PAGE containing natural type I collagen (1 mg/ml) as the substrate.

2.12. RhoA activity assay

RhoA activity was determined by measuring RhoA-GTP binding to glutathione S-transferase-Rhotekin in a pull-down assay (Upstate Cell Signaling, Charlottesville, VA, USA). Briefly, cells were exposed to lysis buffer comprised of 50 mM Tris (pH 7.4), 150 mM NaCl, 10% glycerol, 0.5% NP40, 1 µl/ml aprotinin, 1 µl/ml leupeptin, 1 µl/ml phenylmethylsulfonyl fluoride (PMSF), and 0.5 µl/ml dithiothreitol (DTT), and cellular protein were harvested by scraping with a rubber policeman. Lysates were centrifuged at 4 °C at 12,000 rpm for 5 min to remove particulate material, and protein concentrations were determined by the Bradford assay. Twenty-five micrograms of each protein extract was incubated, rotated at 4 °C for 1 h with an equal volume of GST-Rhotekin-RBD (GST-tagged RhoA-binding domain of the RhoA effector Rhotekin) agarose (Upstate, Biotechnology, Lake Placid, NY, USA), and the samples were washed two times with Mg²⁺ lysis/wash buffer. The RhoA protein was detected by Western blotting with rabbit

anti-RhoA antibody followed by horseradish peroxidase-labeled anti-rabbit antibody. Band intensity was measured from the chemiluminescent signal, and the percent of Rhotekin-bound RhoA (GTP bound active form) was determined for each cell extract.

2.13. Three-dimensional culture

Cancer cells were cultured on a dermal equivalent generated with a Type I-A collagen mixture (Nitta Gelatin, Osaka, Japan) with eight volumes of ice-cold collagen solution, one volume of 10 × reconstitution solution (0.022 g/ml NaHCO₃, 0.0477 g/ml HEPES, 0.05 N NaOH), and one volume 10 × DMEM. A suspension of gingiva fibroblast (1.5 × 10⁵ cells) in culture medium was then added. This mixture was poured onto polycarbonate filter inserts (3 µm pore size, 12 mm diameter; Millipore) and placed in 6-well plates (Costar; Corning, Corning, NY, USA). After 24 h incubation at 37 °C, 3 ml of medium was added to the 6-well plates. Cancer cells (1 × 10⁶ cells) from each cell line were seeded onto the dermal equivalent. After 48 h, the medium in the 6-well plates was changed and fresh culture medium was added to the epidermal equivalent. After 48 h, the cultures were exposed to air by removing the medium from the epithelial layer to generate an air-liquid interface microenvironment. The culture medium was then changed every 2–3 days for 2 weeks. Each culture was performed independently three times and then formalin-fixed, paraffin-embedded, and histologically examined. To measure invasive areas and depth, the culture tissue was stained with hematoxylin and eosin (H&E).

2.14. Xenograft and EGCG treatment

All animal studies were performed in accordance with experimental protocols approved by the animal ethics committee of Yonsei University College of Dentistry. Male Balb/C athymic nude mice (6 weeks of age; the Central Lab Animal, Seoul, Korea) were maintained at 20–22 °C for a 12 h light/dark cycle. Cells (5 × 10⁵ cells/0.1 ml/mouse) were injected submucosally into the tongue within 30 min of harvesting and allowed to establish tumors. Intraperitoneal injection of EGCG began 2 days after tumor cell inoculation. Ten mice with xenografts were randomly divided into the DMSO-treated cancer group and the EGCG-treated cancer group. Each group was injected intraperitoneally (i.p.) every other day with 0.1% DMSO or 20 mg EGCG/0.1% DMSO/kg dose of mice body weight (BW) for 4 weeks. Body weight and tumor mass of the mice were measured twice weekly using a caliper and calculated by the following formula: (width in mm)² × (length in mm)/2. At the end of experiment, the mice were sacrificed by cervical dislocation. Tongues, kidneys, lungs, and livers were harvested, fixed in 4% paraformaldehyde, processed, and embedded in paraffin blocks. Sections were cut to a 4 µm thickness for histopathological evaluation.

2.15. Immunohistochemistry

Serial tissue sections were deparaffinized in xylene, rehydrated in alcohol, and treated with 3% (v/v) H₂O₂ for 10 min at room temperature to suppress endogenous peroxidase activity. Antigen retrieval was conducted with a 10 min autoclave treatment of the sections in 10 mM sodium citrate buffer (pH 6.0). After three rinses with PBS for 5 min each, the sections were incubated with 10% normal goat serum for 20 min at room temperature to block nonspecific binding sites and then reacted for 1 h at room temperature with a primary antibody against phospho/total-Src, FAK, or CTTN, and MT1-MMP, MMP-9, or MMP-2 at a 1:100 dilution in PBS with 1% BSA. The sections were rinsed with PBS and incubated with biotinylated anti-mouse/anti-rabbit IgG (H+L)

(1:100 in PBS with 1% BSA) at room temperature for 30 min, followed by a 30 min exposure to horseradish peroxidase streptavidin (1:200 in PBS with 1% BSA) at room temperature. The sections were reacted with 0.02% 3,3'-diaminobenzidine as the chromogen, counterstained with hematoxylin, dehydrated, and mounted.

2.16. Statistical analysis

The statistical analysis was conducted using InStat™ statistical software (GraphPad Software, Inc., San Diego, CA). Results are expressed as means \pm S.D. Asterisks graphically indicate the statistical significance. The statistical significance of differences between groups was analyzed via repeated measures of one-way ANOVA. $P < 0.05$ were considered significant.

3. Results

3.1. EGCG inhibits invasion of OSCC cells without affecting viability

We first determined the effect of EGCG on Matrigel-coated Transwell cell invasion and motility in YD-10B OSCC cells. EGCG significantly inhibited OSCC cell invasion at doses of 25 and 50 μ M (Fig. 1A). In addition, OSCC cell motility also decreased significantly in the scratch-wound assay following EGCG treatment (Fig. 1B).

These effects were not due to decreased cell viability by EGCG cytotoxicity, as shown by the MTT assay (Fig. 1C). EGCG treatment (0–100 μ M) did not result in a dose- or time-dependent decrease in cell viability at 24 and 48 h. Acquisition of a motile and invasive phenotype is an important step in the development of tumors and ultimately in metastasis. This step involves remodeling of cell-matrix interactions and cell movement mediated by the actin cytoskeleton. Therefore, cell motility and invasion is very dependent on intermediate cell-matrix interaction. To confirm whether EGCG affected OSCC cell ECM adhesion capacity and inhibited migration and invasion, *in vitro* cell adhesion to the ECM was analyzed. As shown in Fig. 1D, no significant different in adhesion capacity was observed on collagen I (Col I), collagen II (Col II), collagen IV (Col IV), fibronectin (FN), laminin (LN), tenascin (TN), and vitronectin (VN) surfaces following EGCG-treatment. We also determined the effects of EGCG on cancer cell invasion and migration by human HSC-3 OSCC. EGCG similarly inhibited the invasion and migration of HSC-3 cells without affecting cell viability or adhesion capacity to the ECM (data not shown).

3.2. EGCG disturbs invadopodia formation and ECM degradation

Staining of the F-actin cytoskeleton in YD-10B OSCC cells resulted in punctuate F-actin-enriched structures at the center and periphery (Phalloidin, red), and these multiple invadopodia foci possessed proteolytic ECM degradation capacity (Fig. 2A).

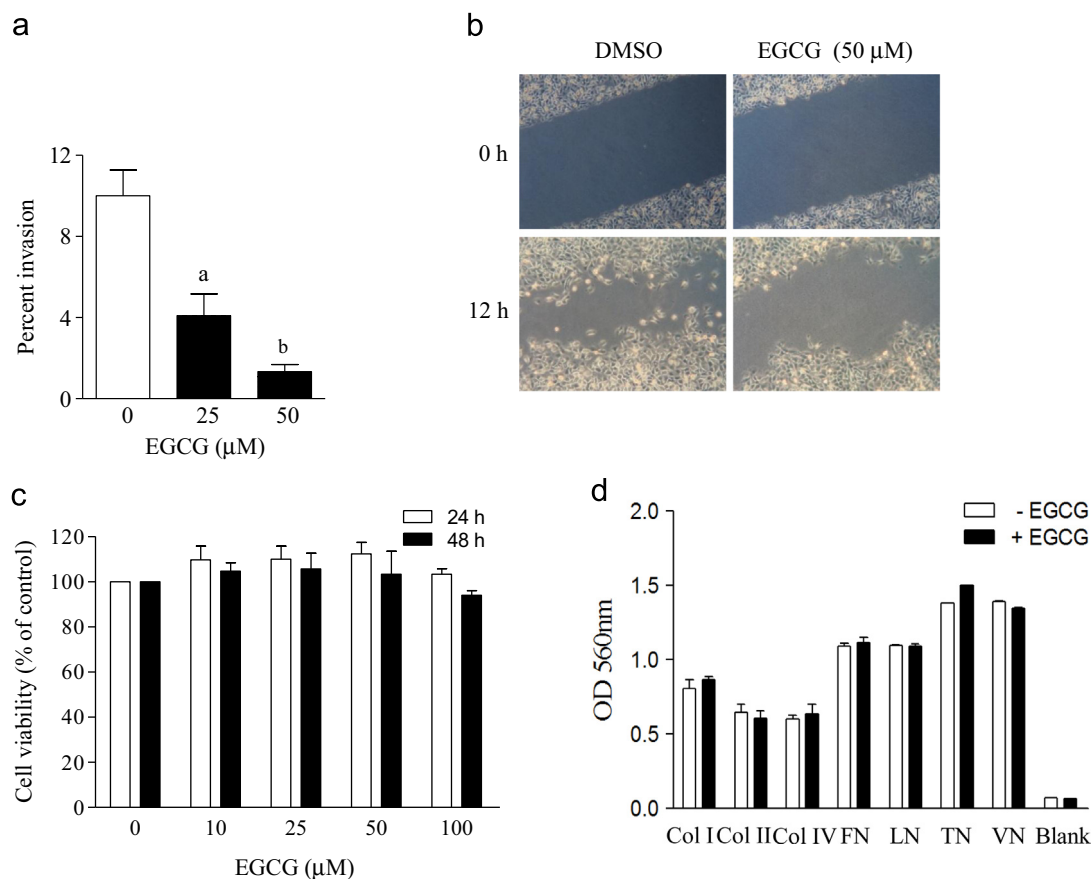


Fig. 1. Epigallocatechin-3 gallate (EGCG) inhibits oral squamous cell carcinoma (OSCC) cell invasion and migration. (A) [3 H]thymidine-labeled YD-10B OSCC cells were incubated in Matrigel-coated Transwell chambers with or without EGCG. Invasion was assessed by radioactivity of the invaded cells and expressed as changes in invasion relative to control conditions. Data are expressed as means \pm S.D. from three independent experiments. ^a $P < 0.05$; ^b $P < 0.001$ versus 0.1% DMSO-treated cells (without EGCG). (B) Confluent OSCC cells monolayers were scraped with a sterile pipette tip, and cells that migrated into the wounded monolayer were captured after 12 h in the presence or absence of EGCG. (C) Cells were cultured in the presence or absence EGCG and cell viability was measured. (D) The cell suspension was incubated on ECM-coated substrates in the presence or absence of EGCG after quenching the trypsin. Bovine serum albumin (BSA)-coated well served as a negative control (Blank). ECM array strip consists of seven different human ECM proteins [collagen I (Col I), collagen II (Col II), collagen IV (Col IV), fibronectin (FN), laminin (LN), tenascin (TN), or vitronectin (VN)]. Data are represented as means \pm S.D. from three independent experiments.

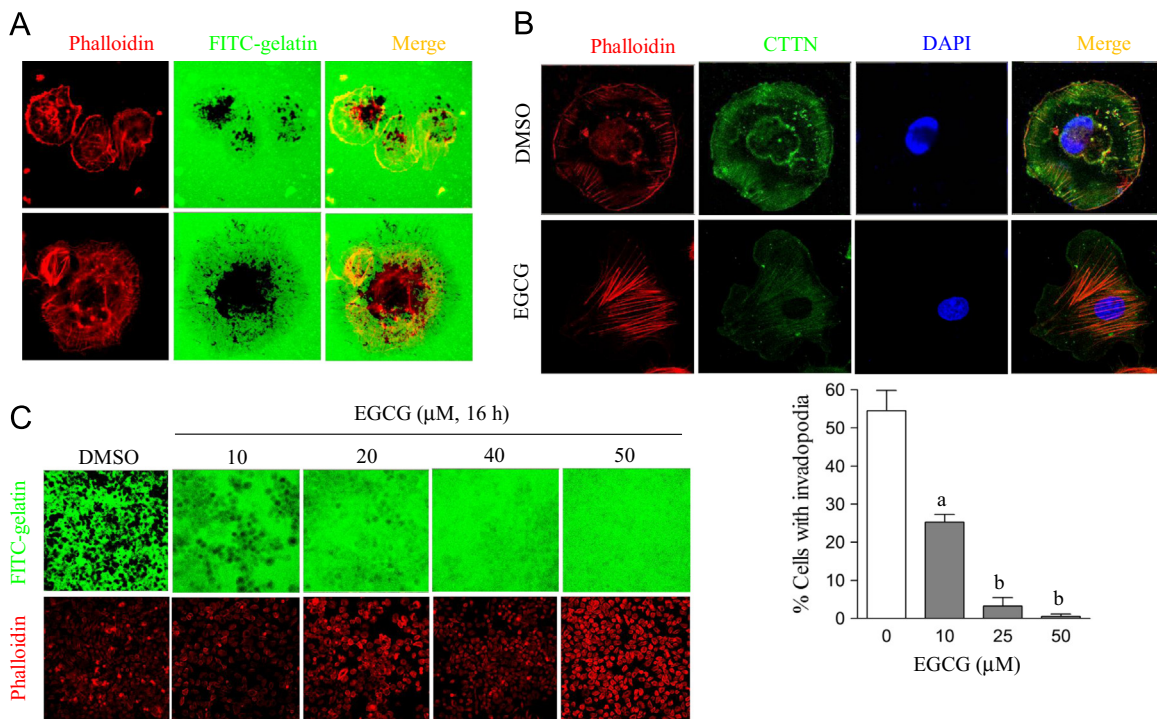


Fig. 2. Epigallocatechin-3 gallate (EGCG) inhibits invadopodia formation and their ECM degradation capacity. (A) Cells were plated on FITC-conjugated gelatin-coated slips (bright green) and then stained with F-actin phalloidin (red). Degraded matrix images were dark areas (lack fluorescence) (original magnification $\times 400$). (B) Cells were plated on gelatin-coated chamber slide, and remaining cells were removed with PBS. After fixation with 4% paraformaldehyde, the cells were labeled to visualize F-actin (phalloidin, red) and cortactin (CTTN, green). The results shown are representative of five independent experiments. (original magnification $\times 400$). Quantified results to determine the percentage of cells that produced invadopodia are presented. ^a $P < 0.05$; ^b $P < 0.001$ versus 0.1% DMSO-treated cells (without EGCG). (C) Cells were plated on FITC-conjugated gelatin-coated slips with or without EGCG. The cells were stained for F-actin with phalloidin (original magnification $\times 100$). (For interpretation of the references to color in this figure legend, the reader is referred to the web version of this article.)

We were interested in whether EGCG influenced invadopodia formation and ECM degradation capacity. As shown in Fig. 2B, fully extended actin fiber bundles without invadopodia were evident on EGCG-treated OSCC cells. ECM degradation capacity was also abolished by EGCG treatment in dose-dependent manner (Fig. 2C). These results indicated that the inhibition of OSCC cell invasion by EGCG may be intimately associated with the disturbance in functional invadopodia formation.

3.3. EGCG inhibits Src, FAK, and CTTN phosphorylation and MMP activity

Signaling initiated by ECM-integrin interactions is transduced to cells by activating integrin-associated FAK and Src. FAK/Src signaling leads to actin cytoskeleton remodeling, which is instrumental during invasion and migration through the ECM. A recent report highlighted that FAK overexpression in esophageal squamous cell carcinoma is correlated with metastasis to lymph nodes and distant organs (Miyazaki et al., 2003). Our Western blot results showed that EGCG attenuated phospho-FAK (Y397) expression in OSCC cells (Fig. 3A). Decreased phospho-FAK (Y397) expression was also observed in the dual staining results with FAK and Phalloidin antibodies against actin by confocal microscopy (Fig. 3B). Src overexpression is common in head and neck squamous cell carcinoma (Koppikar et al., 2008) and is a central element of several signaling pathways regulating adhesion complex formation, actin nucleation, and matrix degradation. Therefore, functional invadopodia are dependent on Src activity, which enhances focal protease secretion for matrix degradation (Murphy and Courtneidge, 2011). As shown in Fig. 3C, phospho-Src (Y416) expression was inhibited by EGCG treatment. Expression of phospho-CTTN (Y466), a downstream molecule of Src, also decreased following EGCG treatment. In addition, MMP-2, MMP-9, and MT1-MMP localized to invadopodia, which mediate focalized proteolysis of the

ECM (Murphy and Courtneidge, 2011). Active Src stimulates MMP-2 and MMP-9 secretion in fibroblasts (Hsia et al., 2003). MT1-MMP carries out the initial cleavage of MMP-2, degrading it to an inactive form during MMP-2 activation (Stanton et al., 1998). Conditioned media from EGCG-treated OSCC cells were assayed for their proteolytic activity to determine the effect of EGCG on MMP secretion. EGCG significantly reduced MMP-2, MMP-9, and MT1-MMP proteolytic activities (Fig. 3D).

3.4. EGCG declines RhoA activity and invasion in 3-D culture

Rho GTPases are also overexpressed in several aggressive cancers and may regulate tumor progression through cytoskeletal organization and contractile events. Evidence suggests that RhoA promotes invadopodia formation by regulating actin dynamics and protease-loaded vesicle docking and exocytosis (Sakurai-Yageta et al., 2008). To determine the effect of EGCG on RhoA activity, we performed a Rhotekin pull-down assay, which has a high affinity for GTP-bound state RhoA, to monitor RhoA protein activation. For representative images, we performed three independent experiments and analyzed them simultaneously. As shown in Fig. 4A, EGCG significantly inhibited RhoA activity compared with that in DMSO-treated OSCC cells. Then, rather than inhibiting RhoA activation by EGCG, we established a dominant-negative RhoA N19-containing stable cell line and observed ECM degradation capacity. Empty vector-containing stable cell (pcDNA 3.1, Mock) displayed multiple invadopodia foci with proteolytic FITC-gelatin degradation capacity, whereas dominant-negative RhoA-containing stable cell (N19) did not create a notable invadopodial spot, indicating suppressed proteolytic matrix degradation (Fig. 4B). In addition, RhoA N19 cells displayed significantly reduced MMP-2, -9, and MT1-MMP activities compared with those of Mock (Fig. 4C). Invasive capability was also assessed by a 3-D

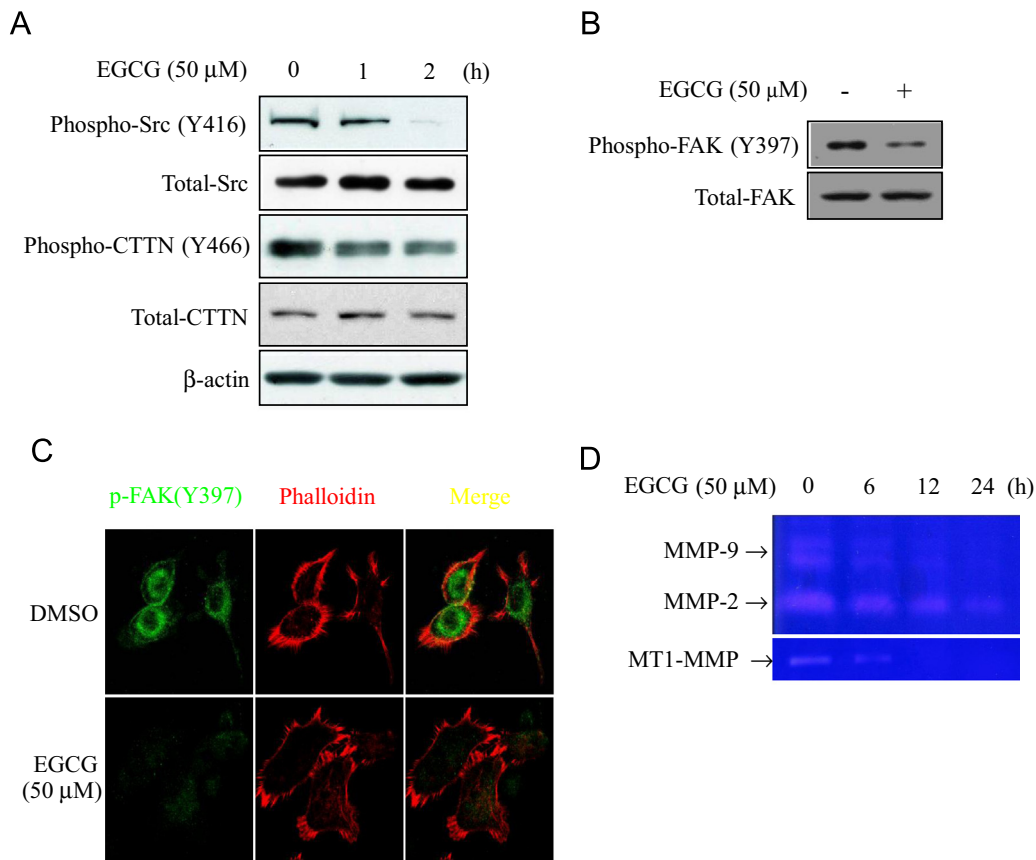


Fig. 3. Epigallocatechin-3 gallate (EGCG) inhibits Src, CTTN, and FAK phosphorylation and MMP activity. (A) Cells were treated with DMSO or EGCG for the indicated times and analyzed by Western blotting with specific antibodies for total/phospho-Src or cortactin (CTTN). β -actin was detected as the loading control. (B) Cells were treated with 0.1% DMSO or EGCG for 2 h. The cells were then lysed, and total protein was analyzed by Western blotting with total or phosphorylation (Y397)-specific antibodies for FAK antibodies. (C) Cells were incubated on collagen-coated chamber slide for 2 h in the presence or absence of EGCG. After fixation, the cells were labeled to visualize F-actin (phalloidin, red) and phospho-FAK (Y397) (green). (D) Cells were treated with EGCG in 1% serum-containing media and maintained for the indicated time. Conditioned medium was harvested, and equal amounts of protein were analyzed by gelatin zymography. For MT1-MMP zymography, the membrane protein extracts were analyzed by 10% SDS-PAGE containing natural type I collagen (1 mg/ml). (For interpretation of the references to color in this figure legend, the reader is referred to the web version of this article.)

cell growth model that mimicked *in vivo* conditions. In Mock cell (wild type), extensive infiltrative growth into the dermal equivalent was observed (white arrows), whereas RhoA N19 cells and EGCG-treated cells (Mock+EGCG) displayed very limited infiltration (Fig. 4D). Meanwhile, HSC-2 cells, which are a low-invasive OSCC cell line, were stably transfected with constitutively active RhoA Q63E (Fig. 4E) and demonstrated increased ECM degradation (Fig. 4F) and cancer cell growth into the dermal equivalent (Fig. 4G). However, these effects were significantly inhibited by the treatment of EGCG. These results indicated that inhibiting RhoA activity by EGCG disrupts invadopodia, thereby abolishing cancer invasion in 3-D culture.

3.5. Anti-tumor effect of EGCG and invadopodia protein expression in orthotopic nude mice

Pathologically, the most common tumor type found in the oral cavity is OSCC. Thus, we tested the effects of EGCG on tumor growth in an orthotopic tumor model. Tumor volume increased remarkably over 4 weeks in mice inoculated with YD-10B OSCC cells (DMSO), but intraperitoneal injections of EGCG significantly inhibited tumor volume (EGCG) in athymic nude mice. (Fig. 5A). H&E staining results indicated that the tongue inoculated tumors were well-differentiated and highly invasive SCC, whereas those of mice supplemented with EGCG were encapsulated. Furthermore, the immunohistochemical analysis indicated that phosphorylated Src, CTTN, and FAK proteins were highly expressed in tumor

tissues of cancer cell-inoculated mice without changes in total protein expression (Fig. 5B). Expression of these proteins was significantly inhibited by EGCG treatment. Expression of MT1-MMP, MMP-9, and MMP-2 in the tumors was also noticeably higher in tumor-inoculated mice, but the expression of these proteins was inhibited by EGCG treatment. These results verified that inhibiting Src by EGCG repressed functional invadopodia formation by inhibiting Src substrate phosphorylation and MMP activities, thereby reducing tumor volume and regional infiltration nearby the stroma in mice. Therefore, EGCG may be a promising anti-invasive agent for OSCC.

4. Discussion

The main finding of our study was that EGCG inhibits functional invadopodia formation and ECM degradation in human OSCC cells, resulting in an anti-invasion effect in an *in vitro* culture system and an *in vivo* mouse model, unlike previous studies that focused on invasive cancer cells.

A better understanding of the mechanisms underlying the metastatic process is essential to develop novel targeted therapeutics. Invadopodia have been increasingly recognized as important drivers of local invasion during metastasis (Caldieri et al., 2009; Yilmaz and Cristofori, 2009). Novel insight into the molecular mechanism of green tea polyphenol-mediated inhibition of cancer invasion is essential to devise preventive and therapeutic approaches.

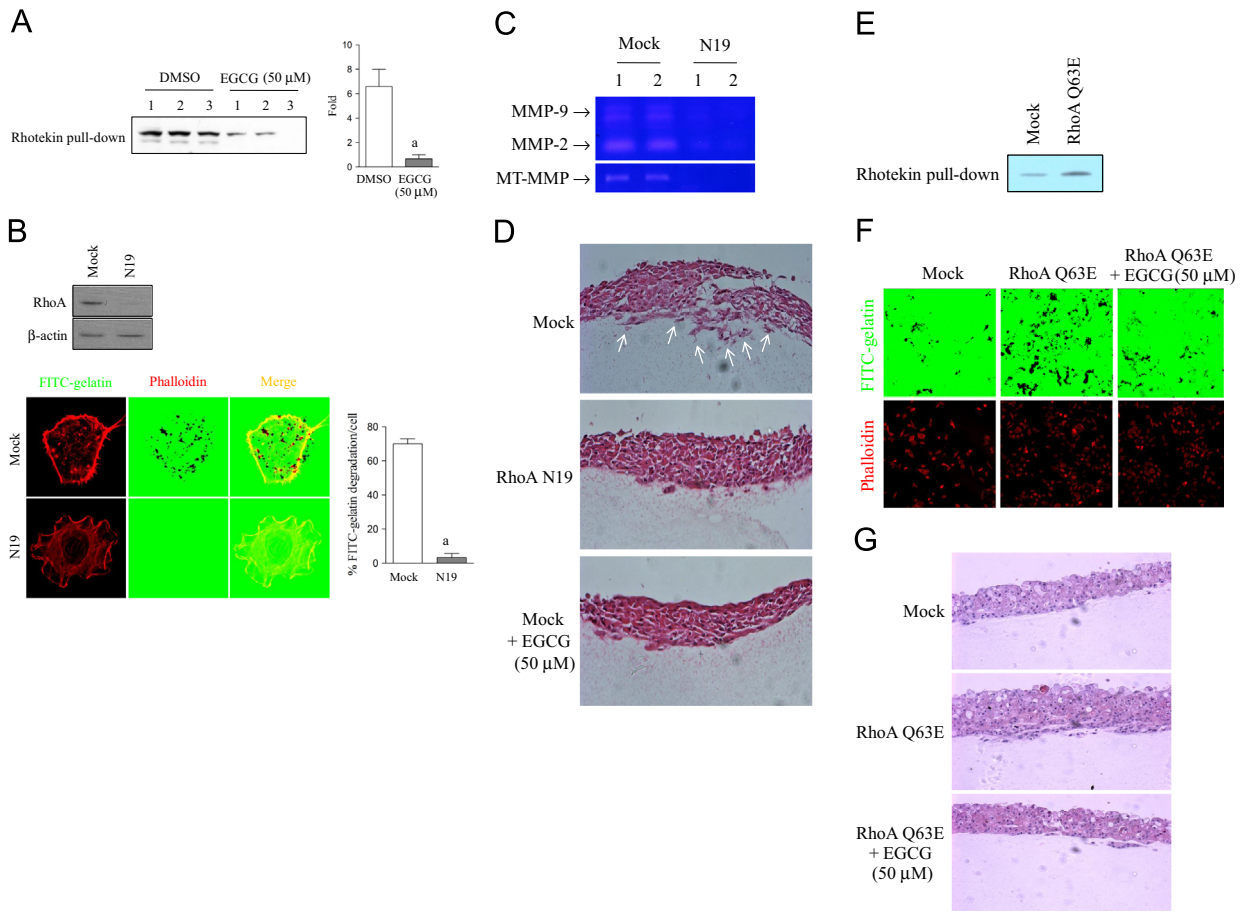


Fig. 4. Epigallocatechin-3 gallate (EGCG) inhibits RhoA activity and invasion in 3-D culture. (A) Cells were treated with DMSO or EGCG for 20 min. RhoA activity was determined by a Rhotekin pull-down assay. Three independent experimental samples from the Rhotekin pull-down assay were analyzed by Western blotting with rabbit anti-RhoA antibody. Band intensity was measured from the chemiluminescence signal, and the percent of Rhotekin-bound RhoA (GTP bound active form) was determined for each cell extract. $^aP < 0.001$ versus non-EGCG-treated cells. (B) The dominant-negative RhoA N19 stable cell line was analyzed for endogenous RhoA level by Western blotting with anti-RhoA antibody. β -actin was detected as the loading control. RhoA N19 cells were cultured on FITC-conjugated gelatin-coated coverslips. Cells were then stained with phalloidin for F-actin. (original magnification $\times 400$). Empty vector-contained stable cells (pcDNA 3.1, Mock) was also analyzed their proteolytic FITC-gelatin degradation capacity. The percentage of FITC-gelatin degradation per the same area in the cell population is shown. $^aP < 0.001$ versus Mock. (C) Mock and dominant-negative RhoA N19 cell-conditioned medium was analyzed via gelatin zymography for MMP-9 and MMP-2 proteolytic activities. The membrane protein extract was also analyzed by type I collagen zymography for MT1-MMP proteolytic activity. We performed three independent experiments and tested each sample in duplicate for every individual test to prepare representative images. (D) Cells were seeded on a dermal equivalent that was generated by a Type I-A collagen mixture. EGCG was added to the culture media and exchanged with fresh medium containing EGCG every 2 days. Invasion of the cells within the dermal equivalent was analyzed by H&E staining. (E) Western blot demonstrating RhoA binding to GST-Rhotekin beads following establishment of constitutively active RhoA Q63E stable cell line with anti-RhoA antibody in low invasive HSC-2 OSCC cell line. (F) Cells were plated on FITC-conjugated gelatin-coated slips with or without EGCG. The cells were stained for F-actin with phalloidin (original magnification $\times 100$). (G) The low invasive HSC-2 Mock cells or constitutively active RhoA Q63E cells were seeded on a dermal equivalent and cultured for 2 weeks in the presence or absence of EGCG.

In the present study, anti-invasion effect of EGCG on OSCC cells was related to the inhibition of functional invadopodia formation, and the resultant loss of their ECM degradation capacity. F-actin staining of OSCC cells revealed punctuate F-actin-enriched multiple spots at the center and periphery, and these multiple invadopodia foci possessed proteolytic ECM degradation capacity. However, fully extended actin fiber bundles without invadopodia were observed on EGCG-treated OSCC cells, indicating that ECM degradation capacity was eliminated. These effects were not due to decreased cancer cell viability or adhesion capacity to the ECM following EGCG treatment. These results potentially indicate that inhibiting OSCC cell invasion by EGCG may be intimately associated with the disturbance in functional invadopodia formation. Meanwhile, as shown in Fig. 2C, the inhibitory effect of EGCG on ECM degradation was found at a concentration lower than its previously known beneficial effective dose. EGCG typically has cellular pharmacological effects at 50–200 μ M *in vitro* cell lines. While FITC-gelatin degradation decreased significantly, even with 10 μ M EGCG treatment, compare with DMSO-treated cells,

FITC-gelatin degradation was almost completely inhibited by 40–50 μ M EGCG. Taking together, the results indicate that EGCG may prevent invasion of OSCC by regulating functional invadopodia formation.

Presently, EGCG treatment resulted in actin cytoskeleton remodeling and decreased FAK, Src, and CTTN phosphorylation. These results provide mechanistic insight into the role of EGCG during inhibition of oral cancer cell invasiveness and motility by eliminating functional invadopodial formation. The initiation of invadopodia formation is largely triggered by engaging cell surface integrins through ECM components (Mueller et al., 1999). Signals initiated by ECM-integrin interactions are transduced into cells through activation of integrin-associated FAK and Src (Guo and Giancotti, 2004). FAK/Src signaling leads to actin cytoskeleton remodeling instrumental for invasion and migration through the ECM. In particular, Src is clearly a central element in the diverse pathways regulating adhesion complex formation, actin dynamics, and matrix degradation. A previously report indicated that cells fail to initiate invadopodia formation and matrix degradation

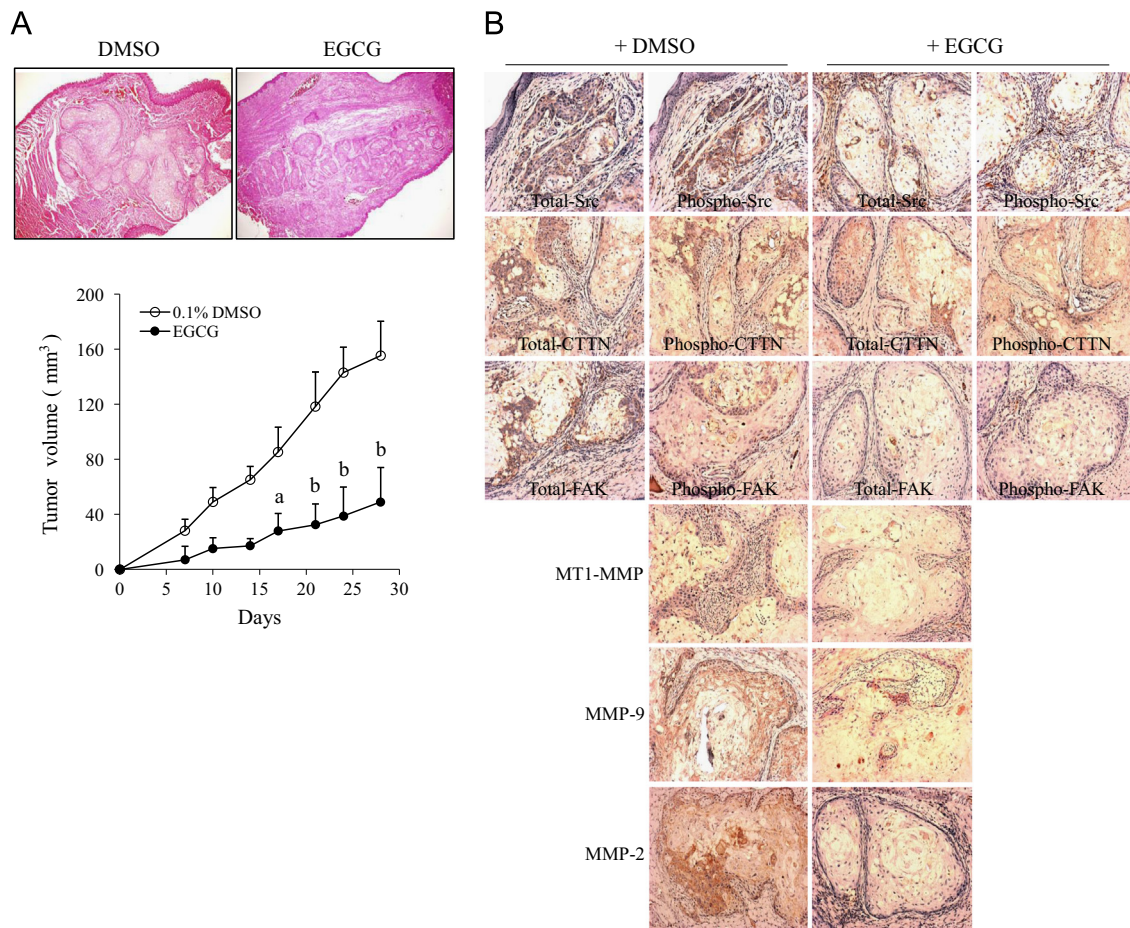


Fig. 5. Epigallocatechin-3 gallate (EGCG) inhibits tumor growth and invadopodia protein expression in athymic nude mice. (A) Cells (5×10^5 cells/0.1 ml/mouse) were injected submucosally into the tongue, and intraperitoneal injections of EGCG began 2 days after inoculation of cells ($n = 10$ /group). H&E staining analysis of tumor from mice inoculated with cancer cells (DMSO) and those of mice supplemented with 20 mg EGCG/kg BW (EGCG) are shown. Tumor volume was calculated. (original magnification $\times 100$). ^a $P < 0.05$; ^b $P < 0.001$ versus 0.1% DMSO-treated cells. (B) An immunohistochemical analysis with the indicated antibodies was performed on tongue tumor tissue sections (original magnification $\times 200$).

when treated with receptor tyrosine kinase (Src) inhibitors (Bowden et al., 1999). Constitutive-active Src is able to stimulate invadopodia formation in fibroblast and carcinoma cells (Artym et al., 2006). Examination of archival oral cancer specimens indicated that enhanced expression of FAK may contribute to the aggressive phenotype of oral cancers (Korberg, 1998). The multi-domain actin-binding protein CTTN is one of the key effector proteins during invadopodia formation. Live cell imaging of c-src-expressing carcinoma cells showed that aggregation of CTTN at the invadopodial initiation site is an early step of invadopodia formation, which is followed by MT1-MMP targeting to these sites and subsequent degradation of underlying matrix substrates (Artym et al., 2006). CTTN has been recently suggested as a predictor of cancer risk in patients with premalignant oral epithelial lesions (deVicente et al., 2012). Our results corroborate the previous finding that tyrosine phosphorylation of CTTN is a commonly utilized downstream indicators for preclinical therapeutic anti-FAK/Src efficacy, because FAK/Src-mediated phosphorylation of CTTN is an important signal enabling tumor invasion and motility (W. Wang et al., 2011). In addition, since CTTN phosphorylation is important for tumor cell motility and ECM degradation at invadopodia (Oser et al., 2010), the CTTN tyrosine phosphorylation status can serve as a downstream monitor of Src activity. Furthermore, the FAK/Src/CTTN axis would be a suitable candidate for potent anti-invadopodia drugs, such as EGCG.

Recruitment of MT1-MMP to preinvadopodia initiates matrix degradation and invadopodia maturation, with further maturation

involving dissolution of the CTTN-F-actin complex, focal retention of MT1-MMP and continued proteolytic activity (Artym et al., 2006). Localization of transmembrane and secreted MMPs to invadopodia involves directed trafficking of vesicles emanating from the trans-Golgi network, where a dynamin-2-N-WASp-Arp2/3-CTTN complex has been implicated in coupling cortical actin regulation with invadopodia membrane dynamics (Buccione et al., 2004). Interestingly, CTTN plays an important role in membrane trafficking that is required for generation and/or fission of vesicles. A recent study has brought novel insights to the function of CTTN in invasion by showing that CTTN might regulate secretion of MT1-MMP and MMP-2 and/or MMP-9 at invadopodia (Clark and Weaver, 2008; Clark et al., 2007). Accordingly Src-mediated phosphorylation may also play a critical role, as tyrosine phosphorylation of CTTN increases invadopodia-mediated ECM degradation.

Rho GTPases regulate cytoskeletal dynamics and migration in many diverse cell types (Heasman and Ridley, 2008). In particular, RhoA GTPase is localized to invadopodial structures and its activity is essential for formation, regulation, and invasive potential in Src-transformed fibroblasts. Inhibiting invadopodia with either C3 toxin or dominant-negative RhoA disrupts the accumulation of F-actin, cortactin, and Fish (Berdeaux et al., 2004). Inhibiting RhoA also dramatically decreases matrix metalloproteinase (MMP) secretion, suggesting that RhoA activity is also required for ECM degradation by invadopodia (Hotary et al., 2006). A novel invadopodia-associated protein, p27RF-RhoA, has been identified through its interaction with MT1-MMP and localization in the

invadopodia (Hoshino et al., 2009). p27RF-RhoA promotes activation of RhoA at invadopodia by sequestering p27(kip1), which, when free, inhibits RhoA activation by RhoGEFs and inhibits metastasis (Besson et al., 2004; Berton et al., 2009). Taken together, RhoA is required for matrix degradation with IQGAP1 and Cdc42 as the exocyst complex component at the leading edge of protrusion (Sakurai-Yageta et al., 2008). In the present study, EGCG reduced RhoA activation level, thereby inhibiting invasive capability into the dermal equivalent in a 3-D cell growth model by disrupting invadopodia formation in human OSCC cells. This result is consistent with the results of dominant-negative RhoA N19 and constitutively active RhoA Q63E cells. Meanwhile, depletion of Cdc42 by RNA interference or overexpression of a constitutively inactive Cdc42 mutant inhibits invadopodia formation in the metastatic MTLn3 adenocarcinoma cell line (Yamaguchi et al., 2005), whereas overexpression of a constitutively active Cdc42 mutant, but not Rac or Rho, promotes dot-like degradation in RPMI17951 melanoma cells (Nakahara et al., 2003). Transfected Cdc42 but not RhoA or Rac, was detected at invadopodia in A375mm melanoma cells by immunofluorescence microscopy. Hence, function of the Rho GTPases subfamily might be cell type dependent.

To confirm *in vitro* anti-invasive activity of EGCG, we estimated the inhibitory effect of EGCG on tumor growth and invadopodia protein expression in oral cancer xenografts of mice. Intraperitoneal injection of EGCG led to a substantial decrease in tumor volume and regional infiltration into nearby stroma in mice. In addition, EGCG significantly inhibited Src, CTTN, FAK, MT1-MMP, MMP-9, and MMP-2 expression in the tumor tissues of mice. These results indicate that EGCG suppressed oral cancer growth and invasion by inhibiting invadopodia protein expression.

In conclusion, EGCG inhibited cancer invasion by disrupting functional invadopodia formation mainly through Src, CTTN, FAK, and RhoA activation in YD-10B human OSCC cells. Administration of EGCG suppressed tumor growth and regional infiltration into nearby stroma in mice. The findings clearly show that EGCG is an effective dietary chemopreventive agent by decreasing functional invadopodia formation in oral cancer. It is possible that targeting the signaling molecules that regulate functional invadopodia formation might be a more effective means to therapeutically inhibit cancer invasion. Therefore, EGCG is a promising invadopodia-targeted anti-invasive agent for developing a potential cancer therapy.

Acknowledgments

This research was supported by the Basic Science Research Program through the National Research Foundation of Korea (NRF) funded by the Ministry of Education, Science and Technology (2012R1A1A2040564).

References

Artym, V.V., Zhang, Y., Seillier-Moisewitsch, F., Yamada, K.M., Mueller, S.C., 2006. Dynamic interactions of cortactin and membrane type 1 matrix metalloproteinase at invadopodia: defining the stages of invadopodia formation and function. *Cancer Res.* 66, 3034–3043.

Berdeaux, R.L., Diaz, B., Kim, L., Martin, G.S., 2004. Active Rho is localized to podosomes induced by oncogenic Src and is required for their assembly and function. *J. Cell Biol.* 166, 317–323.

Berton, S., Belletti, B., Wolf, K., Canzonieri, V., Lovat, F., Vecchione, A., Colombatti, A., Friedl, P., Baldassarre, G., 2009. The tumor suppressor functions of p27(kip1) include control of the mesenchymal/amoeboid transition. *Mol. Cell Biol.* 29, 5031–5045.

Besson, A., Gurian-West, M., Schmidt, A., Hall, A., Roberts, J.M., 2004. p27Kip1 modulates cell migration through the regulation of RhoA activation. *Genes Dev.* 18, 862–876.

Bowden, E.T., Barth, M., Thomas, D., Glazer, R.I., Mueller, S.C., 1999. An invasion-related complex of cortactin, paxillin and PKCmu associates with invadopodia at sites of extracellular matrix degradation. *Oncogene* 18, 4440–4449.

Bowden, E.T., Coopman, P.J., Mueller, S.C., 2001. Invadopodia: unique methods for measurement of extracellular matrix degradation *in vitro*. *Methods Cell Biol.* 63, 613–627.

Buccione, R., Orth, J.D., McNiven, M.A., 2004. Foot and mouth: podosomes, invadopodia and circular dorsal ruffles. *Nat. Rev. Mol. Cell Biol.* 5, 647–657.

Buccione, R., Caldieri, G., Ayala, I., 2009. Invadopodia: specialized tumor cell structures for the focal degradation of the extracellular matrix. *Cancer Metastasis Rev.* 28, 137–149.

Caldieri, G., Ayala, I., Attanasio, F., Buccione, R., 2009. Cell and molecular biology of invadopodia. *Int. Rev. Cell Mol. Biol.* 275, 1–34.

Chen, P.N., Chu, S.C., Kuo, W.H., Chou, M.Y., Lin, J.K., Hsieh, Y.S., 2011. Epigallocatechin-3 gallate inhibits invasion, epithelial-mesenchymal transition, and tumor growth in oral cancer cells. *J. Agric. Food Chem.* 59, 3836–3844.

Clark, E.S., Whigham, A.S., Yarbrough, W.G., Weaver, A.M., 2007. Cortactin is an essential regulator of matrix metalloproteinase secretion and extracellular matrix degradation in invadopodia. *Cancer Res.* 67, 4227–4235.

Clark, E.S., Weaver, A.M., 2008. A new role for cortactin in invadopodia: regulation of protease secretion. *Eur. J. Cell Biol.* 87, 581–590.

de Vicente, J.C., Rodrigo, J.P., Rodriguez-Santamarta, T., Lequerica-Fernández, P., Allonca, E., García-Pedrero, J.M., 2012. Cortactin and focal adhesion kinase as predictors of cancer risk in patients with premalignant oral epithelial lesions. *Oral Oncol.* 48, 641–646.

Guo, W., Giancotti, F.G., 2004. Integrin signalling during tumor progression. *Nat. Rev. Mol. Cell Biol.* 5, 816–826.

Heasman, S.J., Ridley, A.J., 2008. Mammalian Rho GTPases: new insights into their functions *in vivo* studies. *Nat. Rev. Mol. Cell Biol.* 9, 690–701.

Hoshino, D., Tomari, T., Nagano, M., Koshikawa, N., Seiki, M., 2009. A novel protein associated with membrane-type 1 matrix metalloproteinase binds p27(kip1) and regulates RhoA activation, actin remodeling, and matrigel invasion. *J. Biol. Chem.* 284, 27315–27326.

Hotary, K., Li, X.Y., Allen, E., Stevens, S.L., Weiss, S.J., 2006. A cancer cell metalloprotease triad regulates the basement membrane transmigration program. *Genes Dev.* 20, 2673–2686.

Hsia, D.A., Mitra, S.K., Hauck, C.R., Streblov, D.N., Nelson, J.A., Ilic, D., Huang, S., Li, E., Nemerow, G.R., Leng, J., Spencer, K.S., Cheresch, D.A., Schlaepfer, D.D., 2003. Differential regulation of cell motility and invasion by FAK. *J. Cell Biol.* 160, 753–767.

Hwang, Y.S., Hodge, J.C., Sivapurapu, N., Lindholm, P.F., 2006. Lysophosphatidic acid stimulates PC-3 prostate cancer cell Matrigel invasion through activation of RhoA and NF-kappaB activity. *Mol. Carcinogenesis* 45, 518–529.

Khan, N., Afaq, F., Saleem, M., Ahmad, N., Mukhtar, H., 2006. Targeting multiple signaling pathways by green tea polyphenol (-)-epigallocatechin-3-gallate. *Cancer Res.* 66, 2500–2505.

Koppikar, P., Choi, S.H., Egloff, A.M., Cai, Q., Suzuki, S., Freilino, M., Nozawa, H., Thomas, S.M., Gooding, W.E., Siegfried, J.M., Grandis, J.R., 2008. Combined inhibition of c-Src and epidermal growth factor receptor abrogates growth and invasion of head and neck squamous cell carcinoma. *Clin. Cancer Res.* 14, 4284–4291.

Korberg, L.J., 1998. Focal adhesion kinase expression in oral cancers. *Head Neck* 20, 634–639.

Miyazaki, T., Kato, H., Nakajima, M., Sohda, M., Fukai, Y., Masuda, N., Manda, R., Fukuchi, M., Tsukada, K., Kuwano, H., 2003. FAK overexpression is correlated with tumor invasiveness and lymph node metastasis in oesophageal squamous cell carcinoma. *Br. J. Cancer* 89, 140–145.

Mukhtar, H., Ahmad, N., 1999. Green tea in chemoprevention of cancer. *Toxicol. Sci.* 52, 111–117.

Mueller, S.C., Ghersi, G., Akiyama, S.K., Sang, Q.X., Howard, L., Pineiro-Sanchez, M., Nakahara, H., Yeh, Y., Chen, W.T., 1999. A novel protease-docking function of integrin at invadopodia. *J. Biol. Chem.* 274, 24947–24952.

Murphy, D.A., Courtneidge, S.A., 2011. The 'ins' and 'outs' of podosomes and invadopodia: characteristics, formation and function. *Nat. Rev. Mol. Cell Biol.* 12, 413–426.

Nakahara, H., Otani, T., Sasaki, T., Miura, Y., Takai, Y., Kogo, M., 2003. Involvement of Cdc42 and Rac small G proteins in invadopodia formation of RPMI7951 cells. *Genes Cells* 8, 1019–1027.

Oser, M., Mader, C.C., Gil-Henn, H., Magalhaes, M., Bravo-Cordero, J.J., Koleske, A.J., Condeelis, J., 2010. Specific tyrosine phosphorylation sites on cortactin regulate Nck1-dependent actin polymerization in invadopodia. *J. Cell Sci.* 123, 3662–3673.

Ridley, A.J., 2011. Life at the leading edge. *Cell* 145, 1012–1022.

Sakurai-Yageta, M., Recchi, C., Le Dez, G., Sibarita, J.B., Daviet, L., Camonis, J., D'Souza-Schorey, C., Chavrier, P., 2008. The interaction of IQGAP1 with the exocyst complex is required for tumor cell invasion downstream of Cdc42 and RhoA. *J. Cell Biol.* 181, 985–998.

Stanton, H., Gavrilovic, J., Atkinson, S.J., d'Ortho, M.P., Yamada, K.M., Zardi, L., Murphy, G., 1998. The activation of ProMMP-2 (gelatinase A) by HT1080 fibrosarcoma cells is promoted by culture on a fibronectin substrate and is concomitant with an increase in processing of MT1-MMP (MMP-14) to a 45 kDa form. *J. Cell Sci.* 111, 2789–2798.

Wang, H., Bian, S., Yang, C.S., 2011. Green tea polyphenol EGCG suppresses lung cancer cell growth through upregulating miR-210 expression caused by stabilizing HIF-1 α . *Carcinogenesis* 32, 1881–1889.

- Wang, W., Liu, Y., Liao, K., 2011. Tyrosine phosphorylation of cortactin by the FAK-Src complex at focal adhesions regulates cell motility. *BMC Cell Biol.* 12, 49.
- Weaver, A.M., 2006. Invadopodia: specialized cell structures for cancer invasion. *Clin. Exp. Metastasis* 23, 97–105.
- Yamaguchi, H., Lorenz, M., Kempiak, S., Sarmiento, C., Coniglio, S., Symons, M., Segall, J., Eddy, R., Miki, H., Takenawa, T., Condeelis, J., 2005. Molecular mechanisms of invadopodium formation: the role of the N-WASP-Arp2/3 complex pathway and cofilin. *J. Cell Biol.* 168, 441–452.
- Yilmaz, M., Christofori, G., 2009. EMT, the cytoskeleton, and cancer cell invasion. *Cancer Metastasis Rev.* 28, 15–33.